Available online at www.sciencedirect.com
SCIENCE DIRECT®
Journal of Power Sources 133 (2004) 25–31
JOURNAL OF POWER SOURCES
www.elsevier.com/locate/jpowsour

Development of new positive-grid alloy and its application to long-life batteries for automotive industry

Jun Furukawa*, Y. Nehyo, S. Shiga

R&D Division, The Furukawa Battery Co., Ltd, 23-6 Kuidesaku, Shimofunao-machi, Joban, Iwaki-city, Fukushima 972-8501, Japan

Received 31 August 2003; received in revised form 27 November 2003; accepted 10 December 2003

Abstract

Positive-grid corrosion and its resulting creep or growth is one of the major causes of the failure of automotive lead–acid batteries. The importance of grid corrosion and growth is increasing given the tendency for rising temperatures in the engine compartments of modern vehicles. In order to cope with this situation, a new lead alloy has been developed for positive-grids by utilizing an optimized combination of lead–calcium–tin and barium. In addition to enhanced mechanical strength at high temperature, the corrosion-resistance of the grid is improved by as much as two-fold so that the high temperature durability of batteries using such grids has been demonstrated in both hot SAE J240 tests and in field trials in Japan and Thailand. A further advantage of the alloy is its recycleability compared with alloys containing silver. The new alloy gives superior performance in both 12-V flooded and 36-V valve-regulated lead–acid (VRLA) batteries.

Keywords: Automotive lead–acid battery; Corrosion; Growth; High temperature; Lead–calcium–tin–barium alloy; Positive-grid

1. Introduction

A major design of automotive lead–acid battery is the maintenance-free (MF) version, which uses lead–calcium–tin (Pb–Ca–Sn) alloys as grid materials to reduce the need to replenish the electrolyte with water. The MF battery does, however, suffer from short cycle-life due to accelerated positive-grid corrosion at high temperature. Such temperature conditions arise because the underhood environment of modern cars tends to be hotter due to lower bonnet height, compact engine compartments and various devices that are intended to meet today's demands for improved driveability, increased fuel economy, and greater safety.

Corrosion causes creep and growth of the positive-grid, and both phenomena act synergistically to bring about a catastrophic limitation to battery life [1]. After this failure mode had been observed predominantly with expanded wrought alloy grids in the USA during the 1990s [2], Pb–Ca–Sn–Ag alloys [3] began to be used to improve battery durability at high temperatures. This resulted in silver contamination in the lead stream reaching as high as 0.005 wt.% or more, i.e. above the upper limit specified in various industrial standards [4,5]. This is due to the fact that recycled metal accounts for an increasingly greater portion of the lead supply in developed countries, where recycling operations are performed by pyrometallurgical rather than by electro-refining processes.

In order to cope with the above situation, work on alloy development has been conducted and a new alloy composition has been successfully commercialized for long-life automotive batteries [6,7]. Test data for this alloy, together its performance in both conventional 12-V flooded and prototype 36-V valve-regulated lead–acid (VRLA) batteries, are presented in this paper.

2. Experimental

2.1. Alloy specimens

Three types of alloy were used as controls, as shown in Table 1. The optimized combination of Pb–Ca–Sn composition and a small addition of Ba was determined and used in an alloy referred to as C21. The compositions of conventional Ag-added and Ba-added alloys were based on published values [8,9].

The alloy specimens were melted at 500 °C in stainless-steel crucibles and cast in two types of iron mold that were preheated to 150 °C. One mold was rectangular-shaped (200 mm length × 15 mm width × 1.5 mm thickness), while the other was dumbbell-shaped as standardized in JIS Z

* Corresponding author. Tel.: +81-246-43-0089; fax: +81-246-44-6866.
E-mail address: j-furukawa@furukawadenchi.co.jp (J. Furukawa).

0378-7753/$ – see front matter © 2004 Elsevier B.V. All rights reserved.
doi:10.1016/j.jpowsour.2003.12.022

Table 1
Composition of test alloys

Alloy	Composition
Conventional	Pb–0.06 wt.% Ca−1.2 wt.% Sn
C21	Pb–Ca–Sn with Ba
Ag-added	Pb–0.04 wt.% Ca–0.6 wt.% Sn–0.03 wt.% Ag
Conventional Ba-added	Pb–0.06 wt.% Ca–1.6 wt.% Sn–0.016 wt.% Ba

2201. The rectangular casts were cut into 70 mm lengths for use in potentiostatic corrosion tests.

The dumbbell specimens 1.5 mm thick) were subjected to tests of mechanical properties at 100 °C. Chemical analyses were performed by means of the ICP method using ICPS-7500 equipment from Shimazu.

Thermal analysis and electrical conductivity measurements were conducted on the conventional and C21 alloys by means of differential scanning calorimetry (DSC) and the four-probe method, respectively.

2.2. Material tests

2.2.1. Corrosion test

Pre-weighed alloy specimens (70 mm × 15 mm × 1.5 mm) were rinsed with ethanol and then set as anodes in 4.88 M H_2SO_4 with a pure-lead counter electrode and a $Hg|Hg_2SO_4$ reference electrode. The alloys were held at 1350 mV by using a potentio-galvanostat (model HA-151, Hokuto Denko). After termination of the corrosion tests, specimens were treated with alkaline mannitol solution to remove the corrosion products, and then weighed to determine the extent of corrosion. The corrosion products were examined by means of X-ray diffraction (XRD) using Geigerflex Rigaku equipment. The XRD conditions were as follows: target, Cu Kα; voltage, 40 kV; current, 40 mA; scan speed, $4^\circ\,min^{-1}$.

2.2.2. Mechanical strength at high temperature

Dumbbell specimens of the alloys were treated for 50, 100, and 200 h at 100 °C and their yield strength was measured at 25 °C by using a tensile and compression tester (Model TG-20kN, NMB Minebea). The cross-head speed was $1.67 \times 10^{-3}\,mm\,s^{-1}$.

2.2.3. Creep strength

Constant-load rupture tests were conducted to evaluate creep strength at high temperature. The applied stress was 16.5 MPa at 100 °C.

2.2.4. Transmission electron microscopy

In order to investigate the effect of Ba addition on precipitation reactions, alloys C21 with and without Ba were subjected to examination by transmission electron microscopy (TEM). The specimens were prepared by ion-milling thinning, followed by an extractive replica method. The TEM studies were performed with a Philips TECNA1-30 instrument operated at 200 kV. The precipitates were chemically analyzed by EDS (STEM mode).

2.3. Battery tests

The C21 and conventional alloys were book-mold cast for positive-grids. Negative grids were prepared by continuous casting. The grids were processed through a normal plate-making process and assembled into JIS 90D26 size, flooded batteries (12 V), which were then subjected to container formation. For 36-V VRLA performance, 2-V cells were constructed as shown below.

2.3.1. Cycle-life test at 75 °C

The JIS D 5301 cycle-life test was conducted at 75 °C. In effect, this test is the same as the SAE J240 procedure (the so-called 'hot J240 test'). Tear-down analyses were performed to measure the corrosion and growth rates of the alloys, which were calculated as per cycle values for comparative purposes. The corrosion layers on positive-grids were examined by scanning electron microscopy (SEM).

2.3.2. Field-driving tests

In order to accelerate the durability of batteries in the field, taxi-driving tests were conducted in Yokohama, Japan and in Bangkok, Thailand. After certain periods, the batteries were recovered and tear-down analyses were conducted.

2.3.3. 'Mild' hybrid electric vehicle cycle-life test for 36-V VRLA battery

A 36-V battery is required for 42-V PowerNets in 'mild' hybrid electric vehicles (HEVs). In this application, the battery is subjected to start and power-assist discharges, regenerative-braking charges, and idling stop and start, in addition to normal automotive service, viz. start (cranking), lighting and ignition. As an accelerated cycling regime has not yet been standardized, a simplified procedure was adopted with a battery state-of-charge of about 70% [10,11]. The cycle-life performance of 36-V VRLA batteries is very much dependent on temperature, which is due to the small heat capacity of this design of battery. In order to facilitate examination of the alloy effects in the positive-grid, 2-V VRLA cells were constructed with either conventional Pb–Ca–Sn or C21 alloy grids.

3. Results and discussion

3.1. Material evaluation

3.1.1. Physical properties

The liquidus and solidus temperatures of the conventional and C21 alloys are listed, together with electrical conductivities and densities, in Table 2. Given the similarity in the properties of both alloys, the C21 grids were processed by normal procedures [7].

Table 2
Physical properties of conventional and C21 alloys

Properties	Conventional alloy	C21 alloy
Liquidus temperature (°C)	327	326
Solidus temperature (°C)	322[a]	318
Electric conductivity/%ISCS	7.5	7.6
Density (g cm^{-3})	11.2	11.2

[a] Estimated value.

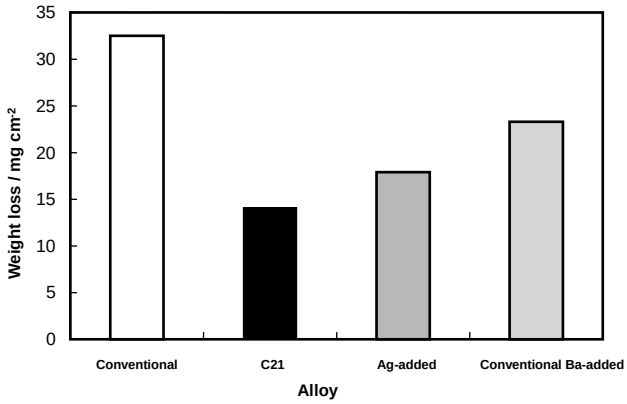

Fig. 1. Comparison of corrosion weight loss of alloys in 1.28 sp. gr. H_2SO_4 after 72 h at constant potential (1350 mV) and 60 °C.

3.1.2. Corrosion

The corrosion rates of the four test alloys at 1350 mV are shown in Fig. 1. The C21 specimen shows a substantially smaller corrosion rate compared with not only the conventional Pb–Ca–Sn, but also with the Ag-added and Ba-added counterparts. In fact, the corrosion-resistance of C21 was twice that of the other three alloys. The relationship between potential and corrosion rate is given in Fig. 2.

The XRD patterns given in Fig. 3 show that at 1000–1200 mV, i.e. a potential range that corresponds to the discharge potential, a large corrosion peak occurs due to

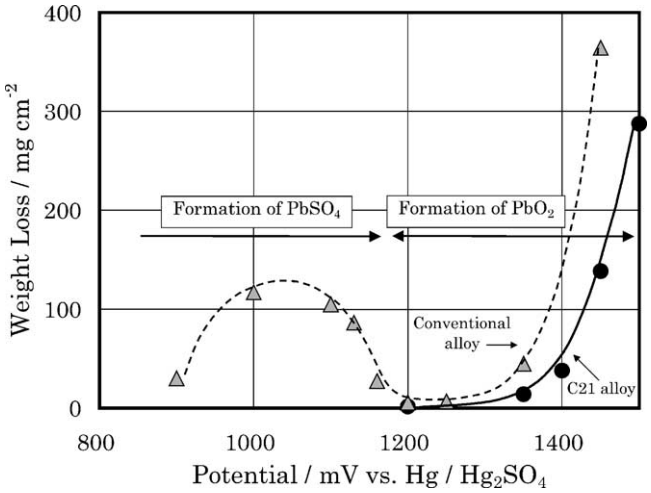

Fig. 2. Relationship between corrosion potential and weight loss for conventional and C21 alloys. Some experimental conditions as in Fig. 1.

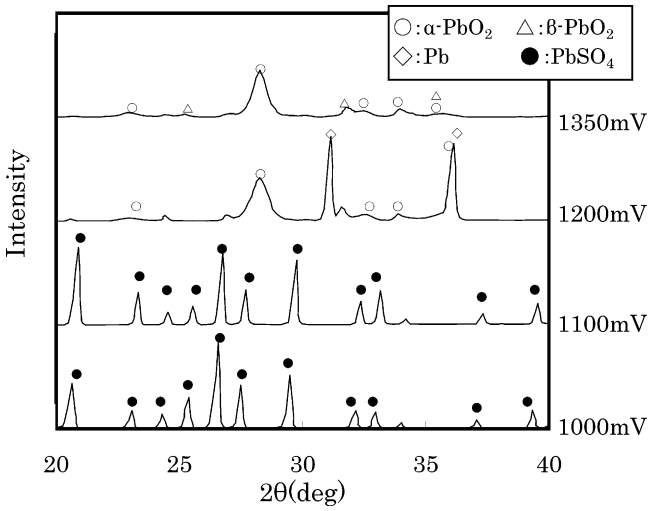

Fig. 3. X-ray powder diffraction patterns of corrosion products on alloys at different potentials.

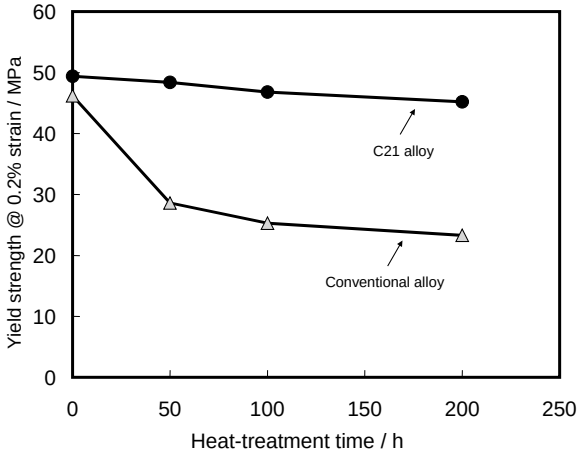

Fig. 4. Comparison of change in yield strength for conventional and C21 alloys at 100 °C.

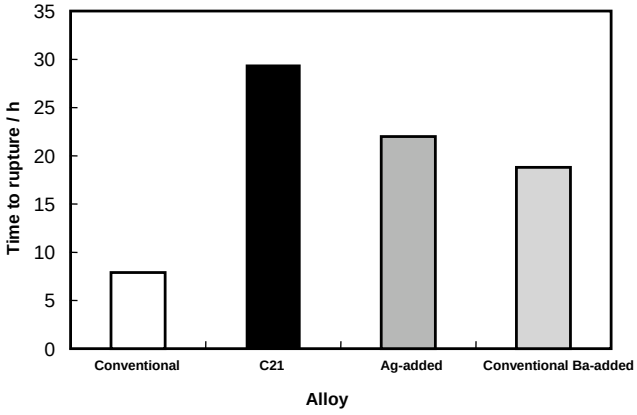

Fig. 5. Comparison of time to rupture of alloys under constant-load creep test at 100 °C.

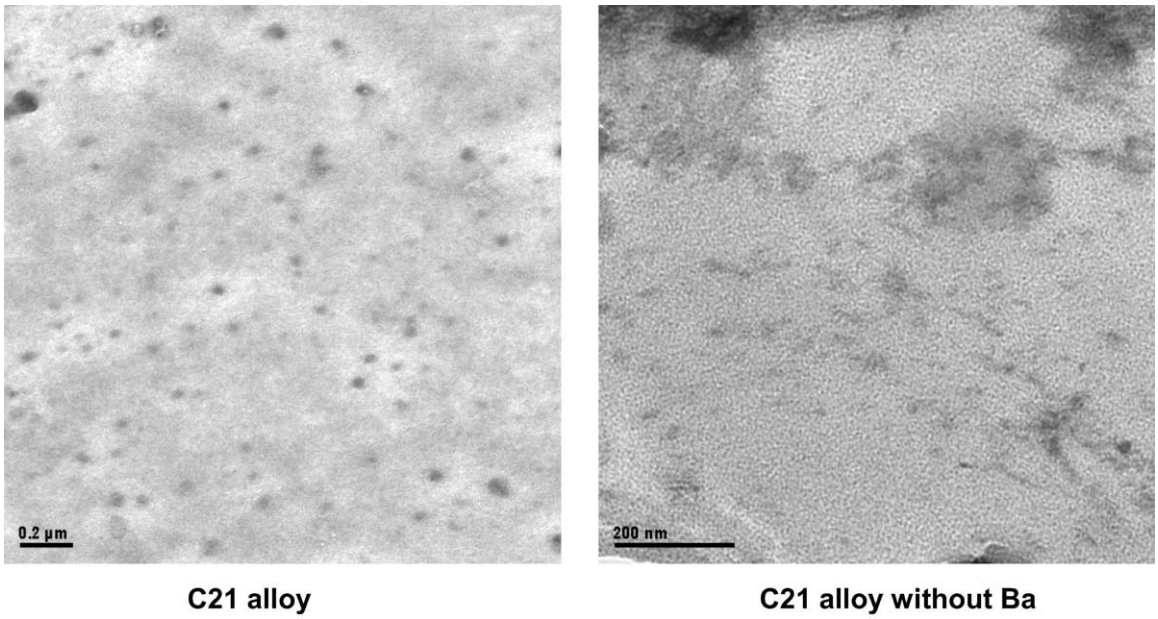

Fig. 6. Comparison of TEM bright field images for C21 and C21 without Ba.

general corrosion formation of $PbSO_4$. A minimum in the corrosion rate is observed at the rest potential (~1200 mV) due to the formation of stable, densely-packed α-PbO_2. At higher potentials, β-PbO_2 begins to appear and the corrosion rate increases. This is probably the result of increased diffusivity in a less-dense film. Thus, alloy C21 displays superior corrosion-resistance under overcharging conditions.

3.1.3. Mechanical properties

Alloy C21 almost maintained its yield strength at 100 °C, even after 200 h. By contrast, the conventional alloy lost strength substantially after only 50 h, which resulted from over-ageing. Constant-load rupture tests showed that the time to rupture for C21 was three times greater than that for conventional alloy, which demonstrates the superior creep strength of C21 (Figs. 4 and 5).

3.1.4. TEM observations

As seen in Fig. 6, there are distinct differences between the two-alloy compositions. In the case of C21 alloy, there is a large population of precipitated particulates. In contrast, there are very few precipitates in the C21 alloy without Ba

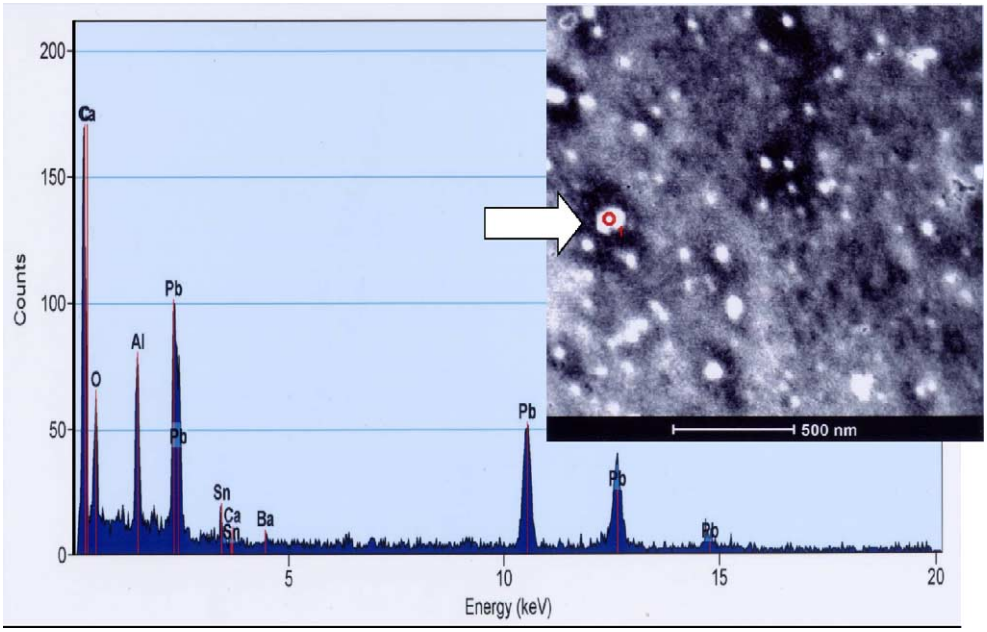

Fig. 7. STEM image and EDS analysis for C21.

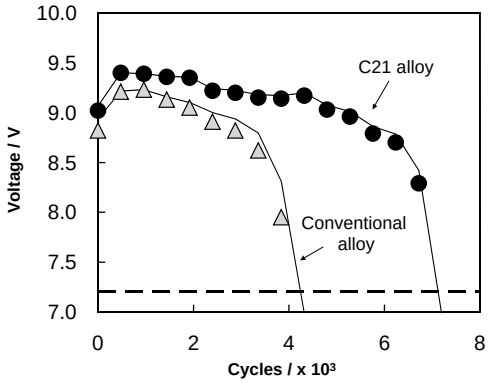

Fig. 8. Battery cycle-life under hot SAE J240 test (test battery: 12-V, JIS-D26 size).

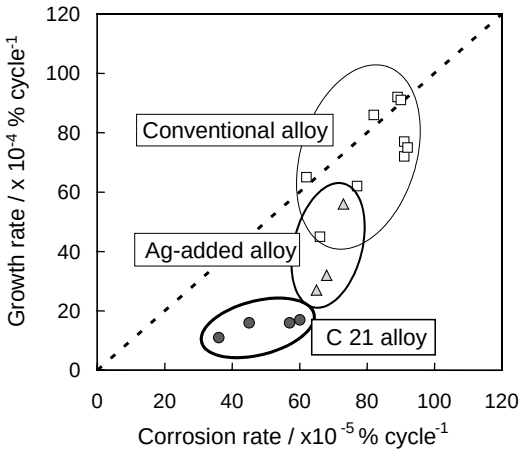

Fig. 10. Relationship between corrosion rate and growth rate of positive-grids under hot SAE J240 test (test battery: 12-V, JIS-D26 size).

addition. EDS analysis of C21 reveals that the precipitates contain Pb–Sn–Ca and Ba elements (Fig. 7). These findings are in accordance with those for the above-mentioned mechanical properties. Barium is a very effective element in promoting the secondary phase formation of fine particulates, which are kept well-dispersed even after a long period at high temperature.

The above observations suggest that corrosion-resistance and creep-resistance act synergistically to suppress the growth rate of the grids and to enhance the high temperature durability of batteries.

3.2. Battery evaluation

3.2.1. Cycle-life at 75 °C

A battery with C21 grids was found to provide good performance for approximately twice as long as a battery with conventional grids (Fig. 8). The appearance of the grids after testing is shown in Fig. 9. It is seen that the C21 grid maintains its original shape substantially, even after a greater period of cycling.

Plots of growth rate as a function of corrosion rate for C21 and conventional alloys are given in Fig. 10. Whereas, the Ag-added alloy displays improved growth properties, the C21 alloy shows enhancement of both corrosion and growth properties.

Electron micrographs of the corrosion layers on conventional and C21 alloys after 2400 cycles are presented in Fig. 11. In the case of the conventional alloy, a thick corrosion layer develops and contains a number of vertical and concentric cracks. These are due to stresses imposed by grid growth as well as by the corrosion layer itself. Lead sulfate is found to be present in many of the cracks, and is considered to be the discharge product of corrosion oxide [12].

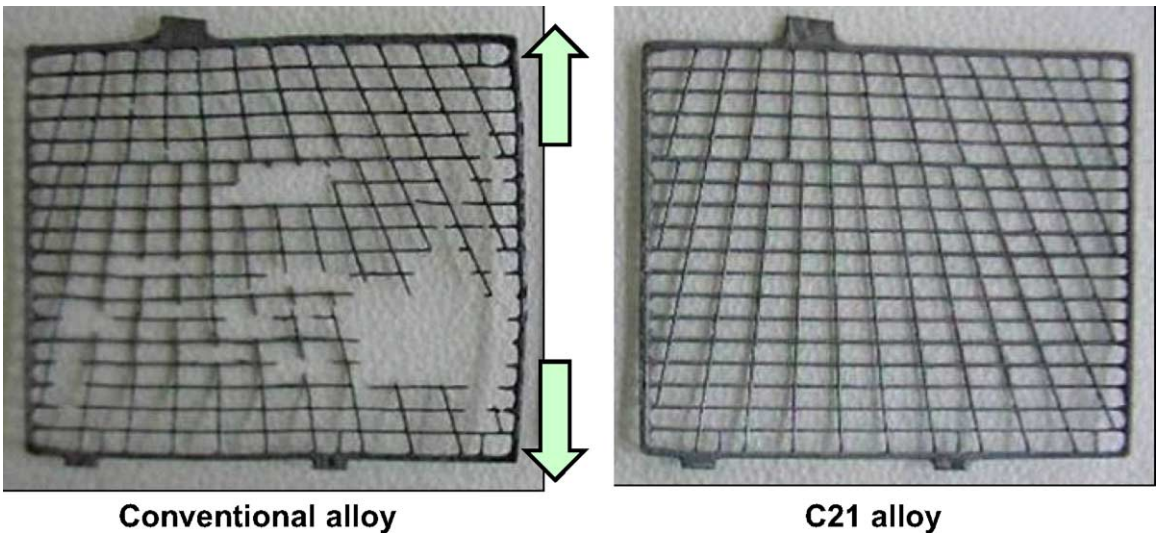

Fig. 9. Appearance of positive-grids after hot SAE J240 test.

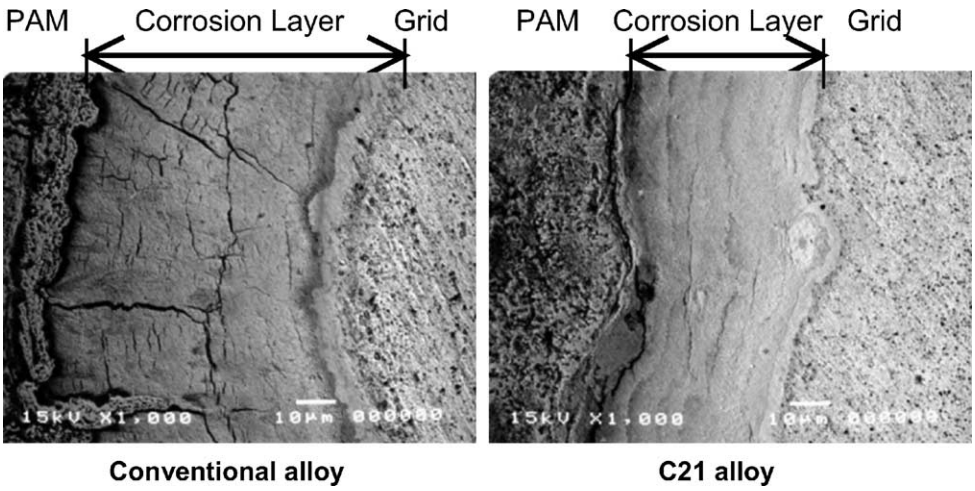

Fig. 11. Electron micrographs of grid|positive active-material interface after 2400 cycles of hot SAE J240 test.

These observations strongly suggest a degradation of the grid|positive active-material interface with increasing electrical resistance. The corrosion layer of C21 is markedly different in that it is thinner, denser and has few cracks. This is due to suppression of growth stresses. The sound interface is believed to maintain good electrical connectivity between the grid and the positive active-material and hence give rise to the high temperature durability of the battery.

3.2.2. Field-driving tests

Taxi-driving tests in Yokohama and Bangkok continued for over 10 months. No failures occurred with batteries that used C21 grids, whereas a few failures were experienced with batteries that used conventional grids. After service, the batteries were recovered and subjected to tear-down analysis

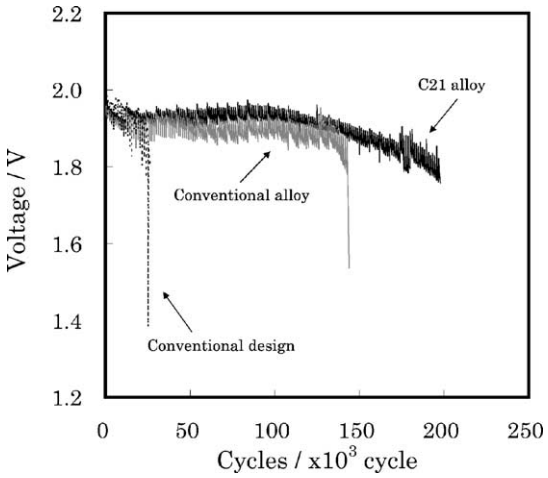

Fig. 12. 'Mild' HEV cycle-life tests at 60 °C (test cell: 2 V, 20 Ah).

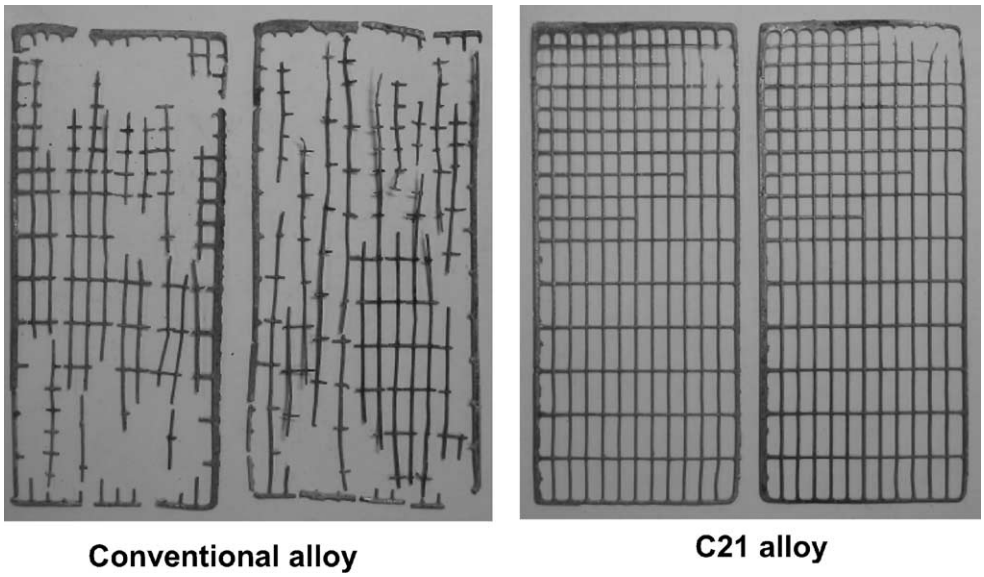

Fig. 13. Condition of positive-grids after 'mild' HEV cycle-life test.

Table 3
Results of taxi-driving tests in Yokohama (Japan) and Bangkok (Thailand)

Positive-grid parameter	Conventional alloy		C21 alloy	
	Bangkok	Yokohama	Bangkok	Yokohama
Weight loss (% per month)	4.1	2.5	2.3	2.0
Growth rate (% per month)	0.54	0.12	0.13	0.04

to examine grid corrosion and growth. The results are presented in Table 3. The corrosion and growth rates of C21 grids were much reduced compared with those of conventional grids, and were more intense in hotter Bangkok. The difference between the two alloys is more remarkable in terms of growth rather than corrosion.

3.2.3. 'Mild' HEV cycle test of 36-V battery

Studies show that cells with C21 grids provide substantially longer cycle-life under the partial state-of-charge (PSoC) duty that is typically experienced in 'mild' HEVs (Fig. 12). The condition of the grids after service is shown in Fig. 13. It is seen that the conventional alloy has become heavily corroded.

4. Conclusions

(i) In order to enhance the cycle-life of automotive batteries at high temperatures, a new alloy, C21, has been developed. This is made with a Pb–Ca–Sn–Ba grid alloy that is optimized to enhance corrosion-resistance and mechanical strength at high temperature and, thereby, provide superior growth-resistance.
(ii) Barium in the C21 alloys acts to promote the precipitation reaction of the Pb–Ca–Sn system.
(iii) 'Hot' SAE J240 tests at 75 °C demonstrate that C21 grids have lower corrosion and growth rates, i.e. about one half (or lower) those of conventional Pb–Ca–Sn grids.
(iv) The C21 alloy is superior to Ag-added alloys, not only in corrosion/growth-resistance but also in recycleability. Thus, use of the new grid would remove the silver accumulation problem in secondary metal streams.
(v) Taxi-driving tests, i.e. accelerated field-driving evaluation, in Japan and Thailand have demonstrated that C21 grids provide superior battery life through enhanced corrosion/growth-resistance.
(vi) Preliminary cell tests for a 36-V VRLA battery have demonstrated that C21 grids can substantially improve PSoC cycle-life.

Acknowledgements

The authors are grateful to Mr. Y. Mori and Mr. T. Hiraki of Toho Zinc Co., Ltd. for collaboration in alloy development, and to Assistant Professor Dr. T. Yasuno of Iwaki Meisei University for TEM studies.

References

[1] A.G. Cannoe, D.O. Feder, R.V. Biagetti, Bell Syst. Technol. J. 49 (1970.9) 1279–1303.
[2] D. Barron, SAE Technical Paper 1999-01-1084 (1999).
[3] R.D. Prengaman, J. Power Sources 78 (1999) 123–129.
[4] M.W. Stevenson, J.E. Manders, S. Eckfeld, R.D. Prengaman, J. Power Sources 107 (2002) 146–154.
[5] R.D. Prengaman, in: Battery International Council 115th Convention, May 18–21, 2003.
[6] Y. Ogata, FB Tech. News 58 (2002) 58.
[7] Y. Nehyo, M. Ozaki, T. Honma, J. Furukawa, S. Niitsuma, FB Tech. News 59 (2003) 8–14.
[8] US Patent 5,298,350, March 17, 1992.
[9] E. Jullian, L. Albert, J.L. Caillere, J. Power Sources 116 (2003) 185–192.
[10] J. Furukawa, H. Sakamoto, H. Iizuka, H. Sho, K. Mashimo, in: Proceedings of the Second Advanced Automotive Battery Conference, February 2002, Las Vegas, NV, USA.
[11] J. Furukawa, H. Sakamoto, H. Iizuka, FB Tech. News 58 (2002) 3–8.
[12] K. Sogabe, J. Furukawa, FB Tech. News 58 (2002) 14–18.